A New Framework for Understanding Recombination-Limited Charge Extraction in Disordered Semiconductors

Kay, Austin M.; Riley, Drew B.; Meredith, Paul; Armin, Ardalan; Sandberg, Oskar

Published in:
Journal of Physical Chemistry Letters

DOI:
10.1021/acs.jpclett.4c00218

Published: 25/04/2024

Document Version
Final published version

THE JOURNAL OF PHYSICAL CHEMISTRY LETTERS
A JOURNAL OF THE AMERICAN CHEMICAL SOCIETY

pubs.acs.org/JPCL
Letter

A New Framework for Understanding Recombination-Limited Charge Extraction in Disordered Semiconductors

Austin M. Kay,* Drew B. Riley,* Paul Meredith, Ardalan Armin, and Oskar J. Sandberg*

Cite This: J. Phys. Chem. Lett. 2024, 15, 4416−4421
Read Online

ACCESS | Metrics & More | Article Recommendations | Supporting Information

ABSTRACT: Recombination of free charges is a key loss mechanism limiting the performance of organic semiconductor-based photovoltaics such as solar cells and photodetectors. The carrier density-dependence of the rate of recombination and the associated rate coefficients are often estimated using transient charge extraction (CE) experiments. These experiments, however, often neglect the effect of recombination during the transient extraction process. In this work, the validity of the CE experiment for low-mobility devices, such as organic semiconductor-based photovoltaics, is investigated using transient drift-diffusion simulations. We find that recombination leads to incomplete CE, resulting in carrier density-dependent recombination rate constants and overestimated recombination orders; an effect that depends on both the charge carrier mobilities and the resistance−capacitance time constant. To overcome this intrinsic limitation of the CE experiment, we present an analytical model that accounts for charge carrier recombination, validate it using numerical simulations, and employ it to correct the carrier density-dependence observed in experimentally determined bimolecular recombination rate constants.

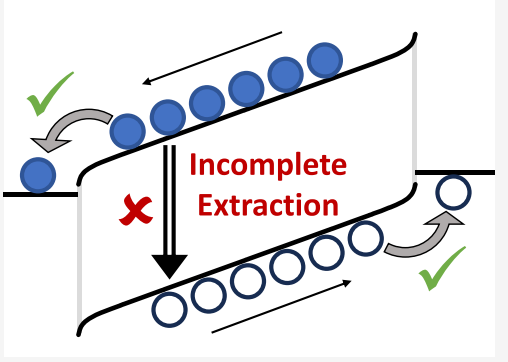

Photovoltaic devices based on next-generation, solution-processable organic semiconductors are—at the time of writing—edging toward commercial viability, particularly in applications such as indoor light harvesting and building-integrated photovoltaics, in which requirements such as band gap tunability are important considerations. With current state-of-the-art power conversion efficiencies (PCEs) of organic solar cells surpassing 19% now regularly reported in the literature,[1−4] minor improvements in device-level and material-level characteristics could pave the way to PCEs above and beyond 20%.[5] Of the several loss mechanisms that currently restrain organic photovoltaics (OPVs), charge carrier recombination of photogenerated electrons and holes is a major limiting factor,[6] giving rise to losses in both the open-circuit voltage and the fill factor.

There exists a repertoire of transient electrical techniques for probing charge carrier recombination in OPVs,[6−15] including transient photovoltage (TPV), charge extraction by linearly increasing voltage (CELIV), time-delayed collection field (TDCF), and transient charge extraction (CE) experiments. CE experiments have, in particular, been widely used to infer the carrier density (n) dependence of the recombination rate ($\mathcal{R}$) in OPVs. It is generally expected that the recombination rate in OPVs is of a bimolecular form $\mathcal{R} \sim \beta n^2 \propto n^{\delta}$, ideally characterized by a carrier density-independent recombination rate constant β and reaction order $\delta = 2$.[16] Despite this, CE experiments have frequently suggested a carrier density-dependence in β that leads to $\delta > 2$, which has commonly been attributed to recombination via trap-like tail states.[17−20] It was recently shown, however, that most electrical techniques (including CE) are detrimentally affected by capacitive effects,[9,21−23] limiting their use at low light illumination intensities. Additionally, at higher intensities such as those characteristic of solar fluxes, CE experiments on thin-film diodes based on low-mobility materials (such as OPVs) may be inadvertently affected by both incomplete CE and limitations set by the RC time; how these effects influence the determination of β and δ is not known.

In this work, we investigate the validity of using transient CE experiments to probe the carrier density-dependence of the charge carrier recombination rate in OPVs. Specifically, we clarify the role of mobility and RC time in the evaluation of β and δ. Indeed, utilizing an open-source, transient drift-diffusion model presented in the Supporting Information,[21,24−27] we find that incomplete CE leads to mobility-dependent and series resistance-dependent bimolecular recombination rates—artifacts that could be falsely interpreted as evidence for higher-order recombination processes. To overcome these limitations, we provide an alternative framework through which CE

Received: January 22, 2024
Revised: April 5, 2024
Accepted: April 10, 2024
Published: April 16, 2024

measurements may be interpreted, before presenting an analytical model for the recombination coefficient obtained through a CE experiment that accounts for incomplete charge transport. We then validate this model against data simulated using the drift-diffusion model, before demonstrating how the model can be used to correct the carrier density-dependence observed in experimental data.

A schematic diagram of the transient CE experiment is illustrated in Figure 1.[21,28] Therein, an OPV device with active

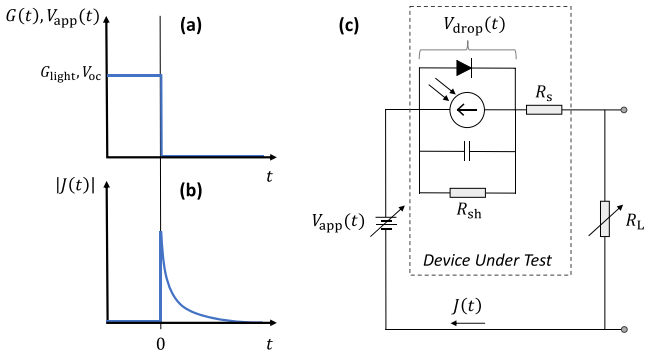

Figure 1. Schematic of the transient CE experiment. (a) As a function of time (t), the generation rate ($G \approx G_{light}$) across the active layer of the OPV device (proportional to the intensity of the light) and the voltage applied to the circuit (V_{app}). The device is kept at open-circuit conditions under steady-state illumination until time $t = 0$, when the light and voltage sources are turned off simultaneously, leading to (b) the extraction of a current density (J) from the device, from which an extracted carrier density may be determined. (c) A circuit diagram illustrating the transient CE experiment, including the equivalent circuit of the OPV device under test (indicated by the dashed box), which is connected in series with a variable voltage source and a variable load resistance.

layer thickness d, electrical cross-sectional area A, shunt resistance R_{sh}, and series resistance R_s is connected in series with (i) a load resistance R_L and (ii) a voltage source that, at a given time t, applies voltage $V_{app}(t)$ to the circuit. The current density $J(t)$ is subsequently obtained by measuring the voltage drop $V_L(t)$ across the load using an oscilloscope ($V_L(t) = J(t)AR_L$). Ideally, R_L and R_s are both assumed to be small enough to not significantly influence the voltage drop $V_{drop}(t)$ across the device during the experiment. Here,

$$V_{drop}(t) = V_{app}(t) - J(t)AR \tag{1}$$

where $R = R_s + R_L$ is the total series resistance of the external circuit. Using this setup, a CE experiment proceeds in two stages.

In the first stage of the CE experiment, the photovoltaic device is kept at open-circuit under steady-state illumination ($V_{app}(t) = V_{drop}(t) = V_{oc}$, the open-circuit voltage). Assuming uniform carrier distributions (i.e., sufficiently high light intensities), the charge carrier recombination rate ($\mathcal{R}_{oc}$) under these conditions relates to the corresponding (open-circuit) carrier density (n_{oc}) within the device via

$$\mathcal{R}_{oc} = \beta(n_{oc})n_{oc}^2 \tag{2}$$

where β may depend on the carrier density. Under these circumstances, the charge carrier recombination rate is perfectly balanced with the (spatially averaged) generation rate (G_{light}): $\mathcal{R}_{oc} = G_{light}$. Hence, for a given light intensity, $\mathcal{R}_{oc}$ may be inferred from the associated generation rate G_{light}.

In the second stage of the CE experiment, which commences at time $t = 0$, the light incident on the device and the voltage applied to the circuit are turned off simultaneously, while the corresponding induced current response $J(t)$ is measured. The current is given by the sum of the spatially averaged conduction (J_c) and displacement (J_d) current densities across the device: $J(t) = J_c(t) + J_d(t)$. By integrating the resulting $J_c(t)$, the extracted carrier density (n_{CE}) may then be evaluated through

$$n_{CE} = \frac{1}{qd}\int_0^\infty J_c(t)\mathrm{d}t = \frac{1}{qd}\left[\int_0^\infty J(t)\mathrm{d}t - C\Delta V_{app}\right] \tag{3}$$

where the right-hand term accounts for the extracted carrier density associated with the displacement current induced by the change in applied voltage (ΔV_{app}), with $C = \frac{\epsilon_r\epsilon_0}{d}$ being the geometric capacitance of the device (ϵ_r and ϵ_0 are the relative permittivity of the OPV material and the vacuum permittivity, respectively). Note that a reverse bias may also be applied at this stage to hasten CE; this method is referred to as bias-assisted charge extraction (BACE).[28] For simplicity, however, we assume that $V_{app}(t > 0) = 0$, and thus $\Delta V_{app} = V_{oc}$. Note that the conclusions made in the following discussion can be, and indeed are, extended to BACE measurements.

In the ideal case that $n_{CE} = n_{oc}$, the CE experiment may be used to directly evaluate n_{oc} at any given light intensity. The recombination rate constant β can then be determined by measuring n_{CE} for a variety of initial light intensities (i.e., varied G_{light}) and assuming the following relationship

$$\beta_{CE} = \frac{\mathcal{R}_{oc}}{n_{CE}^2} \tag{4}$$

while the reaction order is estimated from the slope: $\delta_{CE} = \partial \ln(\mathcal{R}_{oc})/\partial \ln(n_{CE})$. Here, β_{CE} denotes the recombination rate constant obtained from the CE experiment, whereas the steady-state recombination rate, $\mathcal{R}_{oc}$, can either be estimated from the corresponding G_{light} (noting that $\mathcal{R}_{oc} = G_{light}$), e.g., via the saturated photocurrent density $J_{gen} = qG_{light}d$ measured in reverse-bias under steady-state conditions; or in conjunction with a transient photovoltage (TPV) measurement.[21] Equation 4 allows for the detection of any carrier density dependence of β_{CE} (i.e., deviation from bimolecular recombination), along with the associated recombination order. However, Equation 4 relies on the assumptions of uniform carrier distributions (prior to $t = 0$) and complete CE (after $t = 0$). The former is generally violated at low intensities by the manifestation of a capacitance-limited regime.[21−23] The validity of the latter is expected to depend on the electron and hole mobility (μ_n and μ_p, respectively). For materials with low carrier mobilities (like OPVs), the time it takes to extract all excess carriers may, depending on the carrier density, be longer than the prevailing recombination lifetime; under such conditions, a substantial number of carriers will recombine during the extraction process, inevitably resulting in a violation of the underpinning assumption that $n_{CE} = n_{oc}$.

To clarify the influence of carrier mobility on the extracted carrier density, several light intensity-dependent (i.e., carrier density-dependent) CE experiments were simulated using a numerical drift-diffusion model. The results for the case of negligible series resistance ($R = R_s + R_L = 0$), simulated using

https://doi.org/10.1021/acs.jpclett.4c00218
J. Phys. Chem. Lett. 2024, 15, 4416−4421

the parameters summarized in Table S1 in the Supporting Information, are illustrated in Figure 2a. Therein, the input

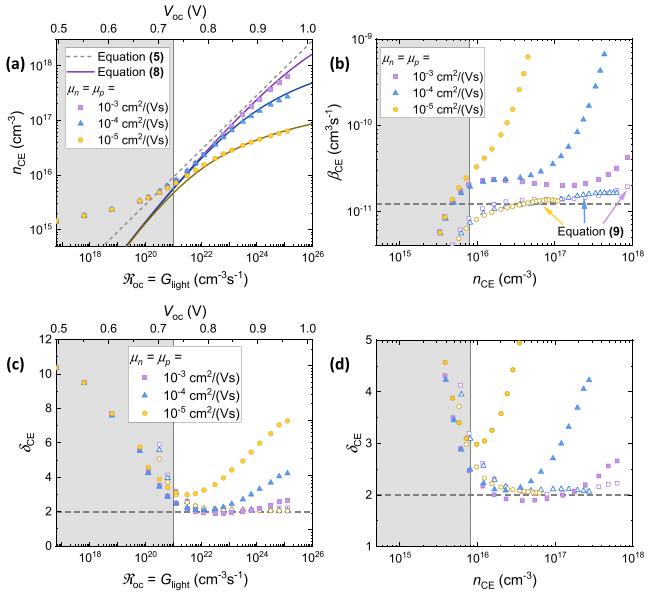

Figure 2. CE measurements simulated in the case of negligible series resistance for a variety of charge carrier mobilities (with $\mu_n = \mu_p$). (a) The extracted carrier density (n_{CE}), plotted as a function of the open-circuit recombination rate $\mathcal{R}_{oc} = G_{light}$. Here, the dashed line indicates the n_{CE} expected from eq 5 in the ideal case that $n_{CE} = n_{oc}$, while the symbols indicate the carrier densities determined by applying eq 3 to simulated current transients. The solid lines indicate the extracted carrier density in the analytical model given by eq 8. For reference, the open-circuit voltage is included as an upper axis, where $qV_{oc} \propto k_B T \ln(G_{light})$. (b) The bimolecular recombination rate constants determined using eq 4 and eq 9 are indicated by filled-in and empty symbols, respectively. The dashed gray line indicates the simulation input value, $\beta = 1.20 \times 10^{-11}$ cm^3 s^{-1}. The corresponding reaction order δ_{CE} is plotted as a function of the recombination rate and the extracted carrier density in (c) and (d), respectively. In all panels, the gray shaded regions at low light intensities/open-circuit voltages indicate approximately where capacitive effects begin to limit the experiment.[21]

recombination coefficient was fixed at $\beta = 1.20 \times 10^{-11}$ cm^3 s^{-1}, corresponding to the case of a purely bimolecular recombination rate ($\delta = 2$). For all results presented in this work, Ohmic contacts were assumed, such that the effects of surface recombination are negligible. From Figure 2a, it is evident that n_{CE} depends on the mobility, especially at higher intensities where lower mobilities were found to correlate with a reduced n_{CE}, consistent with incomplete CE. The resultant bimolecular recombination rate constant determined using Equation 4 is plotted in Figure 2b, and the corresponding recombination order δ_{CE} is plotted against the recombination rate and the extracted carrier density in Figure 2c and 2d, respectively. From Figure 2, it can be seen that the obtained β_{CE} increases with n_{CE}, despite the fact that the input β (shown by the dashed line) was fixed. This, in turn, leads to an overestimation of the recombination order that increases with reduced mobility.

To verify that the apparent variation in β_{CE} with increasing carrier density is indeed an artifact of incomplete CE—and to write a corrected form of eq 4—we next present a simple-yet-accurate analytical model. To simplify the treatment, we assume that the photoactive layer is sufficiently thin, and G_{light} intense enough, for the photogenerated electron and hole density profiles to be essentially flat across the entire active layer in the steady state prior to CE, such that capacitive effects can be neglected.[21] Under these assumptions, the carrier densities of electrons (n) and holes (p) can initially (i.e., at $t \leq 0$) be approximated (at all positions x) as equal to n_{oc}. In accordance with eq 2, we expect

$$n_{oc} = \sqrt{\frac{G_{light}}{\beta}} \tag{5}$$

for purely bimolecular recombination.

Immediately after the light and applied voltage have been turned off ($t > 0$), the sudden change in biasing conditions causes the photogenerated carriers to start drifting under the influence of the electric field induced within the device. In the case of negligible series resistance, the corresponding magnitude of the electric field (F) may be approximated as $F \approx |\Delta V_{app}|/d = V_{oc}/d$. Neglecting diffusive effects, electrons are extracted at $x = d$, moving out of the active layer in a uniform sheet with speed $\mu_n F$, leaving an electron-depleted region of width $l_n(t) = \mu_n F t$ in their wake. At the same time, holes drift as a uniform sheet with velocity $\mu_p F$ in the opposite direction, moving out of the active layer at the contact at $x = 0$ while leaving a hole-depleted region of width $l_p(t) = \mu_p F t$ behind. Thus, the carrier densities can be approximated as $n(x,t) \approx n(t)$ for $x \geq l_n(t)$, and $n(x,t) \approx 0$ elsewhere; while $p(x,t) \approx p(t)$ for $x \leq d - l_p(t)$, and $p(x,t) \approx 0$ elsewhere. During this extraction process, however, recombination between electrons and holes will occur simultaneously within the overlapping region $l_n(t) \leq x \leq d - l_p(t)$ for $t \leq t_{tr}$, where

$$t_{tr} = \frac{d}{(\mu_n + \mu_p)F} \tag{6}$$

After this transit time (when $t > t_{tr}$), the excess electron and hole profiles have no overlap within the active layer, and recombination between them ceases.

Since uniform carrier distributions are assumed at $t = 0$, in the absence of recombination the extracted charge carrier density becomes $n_{CE} = n_{oc}$ in this case. For ohmic contacts, however, there is generally a considerable energy level bending near the contact, suppressing the electron (hole) density near the anode (cathode) in this region. The width of this region is approximately given by the associated Debye screening length $L_D = \sqrt{2\epsilon_r \epsilon_0 k_B T/(q^2 n_{oc})}$.[29] We found that this effect can be accounted for by effectively replacing n_{oc} with $n'_{oc} \approx n_{oc}/\left(1 + \frac{2L_D}{d}\right)$ for small L_D.

The effect of bimolecular recombination during the extraction process can be shown to reduce the extracted carrier density as $n_{CE} = n_{oc} - \int_0^{t_{tr}} \overline{\mathcal{R}}_{CE}(t)\mathrm{d}t$,[15,21] where the spatially averaged recombination rate is given by $\overline{\mathcal{R}}_{CE} = \frac{1}{d}\int_0^d \beta n(x,t)p(x,t)\mathrm{d}x$. On the other hand, as bimolecular recombination diminishes $n(t)$ and $p(t)$ through $\frac{\partial n(t)}{\partial t} = \frac{\partial p(t)}{\partial t} = -\beta n(t)p(t)$, with $n(0) = p(0) = n_{oc}$, this leads to a time-dependent carrier density of the form

$$n(t) = p(t) = \frac{n_{oc}}{1 + \beta n_{oc} t} \tag{7}$$

https://doi.org/10.1021/acs.jpclett.4c00218
J. Phys. Chem. Lett. 2024, 15, 4416−4421

where $\frac{1}{\beta n_{oc}}$ corresponds to the carrier lifetime associated with the bimolecular recombination process. Hence, the extracted carrier density may be written as (see section S1 of the Supporting Information):

$$n_{CE} = \frac{1}{\beta t_{tr}} \ln\left(1 + \frac{\beta n_{oc} t_{tr}}{1 + \frac{2L_D}{d}}\right) \tag{8}$$

where $\beta n_{oc} t_{tr}$ is the ratio between the transit time and the carrier lifetime, which depends on the intensity via n_{oc} through eq 5. Note that, within the logarithm, we have corrected n_{oc} for the Debye screening length to (partially) account for the effect of Ohmic contacts. Accordingly, only when t_{tr} is much shorter than the lifetime associated with bimolecular recombination ($\beta n_{oc} t_{tr} \ll 1$) is there complete CE ($n_{CE} \to n'_{oc}$). However, for low mobilities and/or high light intensities ($\beta n_{oc} t_{tr} > 1$), charge is lost due to recombination during the transient extraction process, leading to $n_{CE} < n_{oc}$. As shown by the close agreement between the drift-diffusion data and the solid lines in Figure 2a, eq 8 reproduces the effect of incomplete CE well.

Using the formula for the corrected n_{CE} given in eq 8, an amended form of the expression for the bimolecular recombination rate constant given in eq 4 can be written as

$$\beta'_{CE} = \sqrt{\beta_{CE}} \times \left[\frac{1}{t_{tr}\sqrt{G_{light}}} \ln\left(1 + \frac{\beta n_{oc} t_{tr}}{1 + \frac{2L_D}{d}}\right)\right] \tag{9}$$

Using eq 9, the extracted bimolecular recombination rate constants previously plotted as solid symbols in Figure 2b were corrected, with the amended values plotted in the same panel as empty symbols. The corrected reaction orders are plotted against $\mathcal{R}_{oc}$ and n_{CE} in Figure 2c and 2d, respectively. Indeed, for all mobilities the obtained β'_{CE} values are within a factor of 2 from the simulation input value ($\beta = 1.2 \times 10^{-11}$ cm^3 s^{-1}), giving a reaction order $\delta_{CE} \approx 2$ for most light intensities. Compared with the orders-of-magnitude fluctuations and apparent n_{CE}-dependence that was observed in β_{CE} for the uncorrected case, it is clear that incomplete CE can lead to erroneous evaluations of the bimolecular recombination rate constant. However, such variations are not an intrinsic limitation of the CE experiment. The fault instead lies with the analysis and the $n_{CE} = n_{oc}$ assumption that underpins eq 4. While the β'_{CE} values determined using eq 9 are far more accurate than the β_{CE} values determined using eq 4, there are still fluctuations in the corrected data points; these are likely due to additionally complexities, such as inhomogeneities in the carrier density profiles,[16,21] which are neglected in the analytical model.

A similar incomplete CE phenomenon may be observed when accounting for the resistance−capacitance (RC) effects that arise from the combined series resistance of the circuit ($R = R_s + R_L$). As demonstrated by the simulations shown in Figure 3a, which were simulated using device area $A = 0.1$ cm^2, increasing the series resistance leads to reduced CE at higher light intensities. This, in turn, leads to an apparent increase in the bimolecular recombination rate constant, as shown in Figure 3b. Ultimately, this culminates in an overestimation of the reaction order, as illustrated by the curves in Figure 3c and 3d. The influence of RC effects is explored further for varied A in Figure S1 of the Supporting Information. Primarily, this effect can be attributed to resistive voltage losses induced by

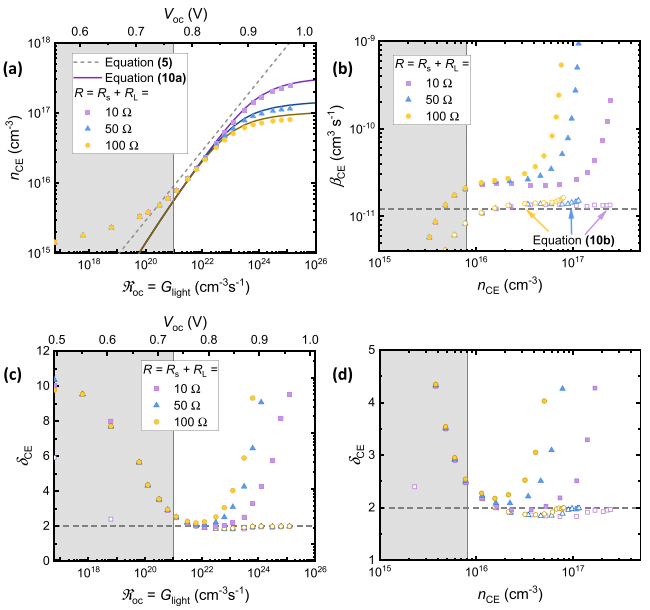

Figure 3. Simulated CE measurements for a device with area $A = 0.1$ cm^2, where the combined series resistances of the circuit ($R = R_s + R_L$) has been varied while the mobility was fixed at $\mu = 10^{-3}$cm^2/(Vs). (a) The extracted carrier density (n_{CE}), plotted as a function of the open-circuit recombination rate $\mathcal{R}_{oc} = G_{light}$. Here, the symbols indicate n_{CE} determined by applying eq 3 to the simulated current transients, the dotted line indicates eq 5, and the solid lines indicate eq 10a. (b) The corresponding bimolecular recombination rate constants determined using eq 4 and 10b are illustrated by the filled-in symbols and empty symbols, respectively. The dashed gray line indicates the simulation input value, $\beta = 1.20 \times 10^{-11}$ cm^3 s^{-1}. The resultant recombination order, determined using $\delta_{CE} = \frac{\partial \ln(\mathcal{R}_{oc})}{\partial \ln(n_{CE})}$, is plotted as a function of the open-circuit recombination rate and the extracted carrier density in (c) and (d), respectively. In all panels, the gray shaded regions at low light intensities/open-circuit voltages illustrate where capacitive effects begin to limit the experiment.[21]

the large extraction current (present at high intensities), reducing the electric field across the device as $F(t) \approx |\Delta V_{app} - ARJ(t)|/d = |V_{oc} - ARJ(t)|/d$. After accounting for resistive losses dominate, such that the RC time $\tau_{RC} = ARC \neq 0$, we find that the extracted carrier density and corrected bimolecular recombination rate constant, denoted as n_{CE}^{RC} and β_{CE}^{RC}, respectively, can be analytically approximated with (see section S2 of the Supporting Information)

$$n_{CE}^{RC} = n_{oc} \times f \tag{10a}$$

$$\beta_{CE}^{RC} = \beta_{CE} \times f^2 \tag{10b}$$

$$f = \frac{1}{\beta n_{oc} t_{tr}} \left[\frac{t_{tr} - t_{tr}^{eff}}{\tau_\beta + t_{tr}^{eff}} + \left(1 + \frac{\frac{\beta_L}{\beta}\tau_{RC}}{\tau_\beta + t_{tr}^{eff}}\right) \ln\left(1 + \frac{t_{tr}^{eff}}{\tau_\beta + \frac{\beta_L}{\beta}\tau_{RC}}\right)\right] \tag{10c}$$

where f is a correction factor, $\tau_\beta = \left(1 + \frac{2L_D}{d}\right)/\beta n_{oc}$ is the recombination lifetime (including the Debye screening factor), $\beta_L = q(\mu_n + \mu_p)/\epsilon_r \epsilon_0$ is the Langevin recombination rate constant, and t_{tr}^{eff} is the effective transit time, which can be approximated (see Supporting Information) as

https://doi.org/10.1021/acs.jpclett.4c00218
J. Phys. Chem. Lett. 2024, 15, 4416−4421

$$t_{tr}^{eff} \approx \left(1 + \frac{\tau_\beta}{\frac{\beta_L}{\beta}\tau_{RC}}\right)\left(\sqrt{\tau_\beta^2 + \frac{2\beta_L}{\beta}\tau_{RC}t_{tr}} - \tau_\beta\right) \quad (11)$$

As expected, in the limit that $R \to 0$, the analytical expressions for the extracted carrier density and the bimolecular recombination rate constant given in eq 10 reduce to eqs 8 and 9, respectively. Eq 10 was used to simulate the solid lines in Figure 3a, as well as the empty data points in Figure 3b. From this figure, one can see that accounting for the combined series resistance of the external circuit is a necessity to accurately determine β.

Finally, to demonstrate how resistances can lead to incomplete CE and possibly an apparent carrier density-dependence in the obtained bimolecular recombination rate constant, we applied the analytical model described by eq 10 to BACE measurements made by Hosseini et al. to correct the experimentally determined bimolecular recombination rate constants of two OPV donor:acceptor blends. Both blends used a naphtho[1,2-c:5,6-c′]bis([1,2,5]thiadiazole)-based polymer (NT812) as the donor.[28,30] While one blend used ITIC as the acceptor, the other used $PC_{70}BM$ (for chemical definitions, see Table S2 in the Supporting Information).[28] Note that a nonzero voltage bias was accounted for in the following calculations (see section S2 of the Supporting Information). By developing and applying an open-source computational tool that employs a least-squares method to estimate β (freely available online; see Supporting Information),[31] we found the carrier density-dependence observed in the β_{CE} data plotted in Figure 4 can be corrected for if we

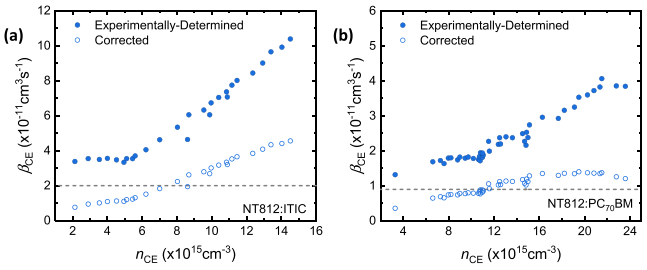

Figure 4. Using the analytical model for CE to correct experimentally determined bimolecular recombination rate constant measurements of an OPV device with (a) an NT812:ITIC active layer and (b) an NT812:PCBM active layer. Here, the filled-in data points represent the experimentally determined bimolecular recombination rate constant, determined as a function of the carrier density using BACE measurements (where $V_{app}(t > 0) \neq 0$) by Hosseini et al.[28] The empty data points indicate the corresponding corrected bimolecular recombination rate constants.

effectively assume $R = 1000\ \Omega$, suggesting that such variations could be described by incomplete CE, rather than higher-order ($\delta > 2$) recombination processes. The trend in β'_{CE} versus n_{CE} observed in Figure 4 now reflects that seen in Figures 2b and 3b. In particular, the large increase in measured β_{CE} has been tempered with a smaller rise followed by a fall. Note that the parameters used to correct this data are provided in Table S3 in the Supporting Information, alongside an expression for the resistance-dominated voltage at $t \ll \tau_{RC}$.

In conclusion, we have developed a simple analytical model to describe CE experiments. By applying this model to drift-diffusion and experimental data, we have shown that bimolecular recombination of excess charge carriers during the transient extraction process of a CE experiment generally leads to incomplete CE in diode devices such as OPVs with low carrier mobilities. This, in turn, may result in an erroneous evaluation of the bimolecular recombination rate constant and an overestimation of the recombination order in low-mobility diodes. To overcome these underlying limitations of the CE experiment, we have presented a new framework for analysis as well as a computational tool[31] for correcting the bimolecular recombination rate constant obtained from experimentally determined CE measurements. We have demonstrated how this model can be applied by correcting the carrier density-dependence of published bimolecular recombination rate data for OPV devices, demonstrating that the technique and computational tool can be used to reinterpret existing measurements in the literature.

■ ASSOCIATED CONTENT

Data Availability Statement

The data that support the results of this work will be made available upon request from the corresponding authors.

Supporting Information

The Supporting Information is available free of charge at https://pubs.acs.org/doi/10.1021/acs.jpclett.4c00218.

Additional simulations, derivations, and descriptions of parameter extraction; a complete description of the drift-diffusion model and an accompanying, open-source computational tool with an accessible graphical user interface. (PDF)

Transparent Peer Review report available (PDF)

■ AUTHOR INFORMATION

Corresponding Authors

Austin M. Kay − *Sustainable Advanced Materials (Sêr-SAM), Centre for Integrative Semiconductor Materials (CISM), Department of Physics, Swansea University Bay Campus, Swansea SA1 8EN, United Kingdom;* orcid.org/0000-0002-9126-5340; Email: a.m.kay.954708@swansea.ac.uk

Drew B. Riley − *Sustainable Advanced Materials (Sêr-SAM), Centre for Integrative Semiconductor Materials (CISM), Department of Physics, Swansea University Bay Campus, Swansea SA1 8EN, United Kingdom;* orcid.org/0000-0001-6688-0694; Email: d.b.riley@swansea.ac.uk

Oskar J. Sandberg − *Physics, Faculty of Science and Engineering, Åbo Akademi University, 20500 Turku, Finland;* orcid.org/0000-0003-3778-8746; Email: oskar.sandberg@abo.fi

Authors

Paul Meredith − *Sustainable Advanced Materials (Sêr-SAM), Centre for Integrative Semiconductor Materials (CISM), Department of Physics, Swansea University Bay Campus, Swansea SA1 8EN, United Kingdom*

Ardalan Armin − *Sustainable Advanced Materials (Sêr-SAM), Centre for Integrative Semiconductor Materials (CISM), Department of Physics, Swansea University Bay Campus, Swansea SA1 8EN, United Kingdom;* orcid.org/0000-0002-6129-5354

Complete contact information is available at: https://pubs.acs.org/10.1021/acs.jpclett.4c00218

Notes

The authors declare no competing financial interest.

https://doi.org/10.1021/acs.jpclett.4c00218
J. Phys. Chem. Lett. 2024, 15, 4416−4421

■ ACKNOWLEDGMENTS

This work was funded through the Welsh Government's Sêr Cymru II Program 'Sustainable Advanced Materials' (Welsh European Funding Office − European Regional Development Fund). P.M. is a Sêr Cymru II Research Chair and A.A. was a Rising Star Fellow also funded through the Welsh Government's Sêr Cymru II 'Sustainable Advanced Materials' Program (European Regional Development Fund, Welsh European Funding Office, and Swansea University Strategic Initiative). This work was also funded by the UKRI through the EPSRC Program Grant EP/T028513/1 Application Targeted and Integrated Photovoltaics and the UKRI Research England RPIF Programme (Centre for Integrative Semiconductor Materials). O.J.S. is an Academy Research Fellow and acknowledges funding from the Research Council of Finland through project #357196.

■ REFERENCES

(1) Liu, S.; Yuan, J.; Deng, W.; Luo, M.; Xie, Y.; Liang, Q.; Zou, Y.; He, Z.; Wu, H.; Cao, Y. High-Efficiency Organic Solar Cells with Low Non-Radiative Recombination Loss and Low Energetic Disorder. *Nat. Photonics* **2020**, *14* (5), 300−305.

(2) Wang, C.; Ma, X.; Shen, Y.-f.; Deng, D.; Zhang, H.; Wang, T.; Zhang, J.; Li, J.; Wang, R.; Zhang, L. Unique Assembly of Giant Star-Shaped Trimer Enables Non-Halogen Solvent-Fabricated, Thermal Stable, and Efficient Organic Solar Cells. *Joule* **2023**, *7*, 2386.

(3) Han, C.; Wang, J.; Zhang, S.; Chen, L.; Bi, F.; Wang, J.; Yang, C.; Wang, P.; Li, Y.; Bao, X. Over 19% Efficiency Organic Solar Cells by Regulating Multidimensional Intermolecular Interactions. *Adv. Mater.* **2023**, *35* (10), No. 2208986.

(4) Zhu, L.; Zhang, M.; Xu, J.; Li, C.; Yan, J.; Zhou, G.; Zhong, W.; Hao, T.; Song, J.; Xue, X.; et al. Single-Junction Organic Solar Cells with Over 19% Efficiency Enabled by a Refined Double-Fibril Network Morphology. *Nat. Mater.* **2022**, *21* (6), 656−663.

(5) Armin, A.; Li, W.; Sandberg, O. J.; Xiao, Z.; Ding, L.; Nelson, J.; Neher, D.; Vandewal, K.; Shoaee, S.; Wang, T.; et al. A History and Perspective of Non-Fullerene Electron Acceptors for Organic Solar Cells. *Adv. Energy Mater.* **2021**, *11* (15), No. 2003570.

(6) Lakhwani, G.; Rao, A.; Friend, R. H. Bimolecular Recombination in Organic Photovoltaics. *Annu. Rev. Phys. Chem.* **2014**, *65*, 557−581.

(7) Pivrikas, A.; Sariciftci, N. S.; Juška, G.; Österbacka, R. A Review of Charge Transport and Recombination in Polymer/Fullerene Organic Solar Cells. *Progress in Photovoltaics: Research and Applications* **2007**, *15* (8), 677−696.

(8) Nyman, M.; Sandberg, O. J.; Österbacka, R. 2D and Trap-Assisted 2D Langevin Recombination in Polymer: Fullerene Blends. *Adv. Energy Mater.* **2015**, *5* (5), No. 1400890.

(9) Azzouzi, M.; Calado, P.; Telford, A. M.; Eisner, F.; Hou, X.; Kirchartz, T.; Barnes, P. R. F.; Nelson, J. Overcoming the Limitations of Transient Photovoltage Measurements for Studying Recombination in Organic Solar Cells. *Solar RRL* **2020**, *4* (5), No. 1900581.

(10) Bartesaghi, D.; Pérez, I. D. C.; Kniepert, J.; Roland, S.; Turbiez, M.; Neher, D.; Koster, L. J. A. Competition Between Recombination and Extraction of Free Charges Determines the Fill Factor of Organic Solar Cells. *Nat. Commun.* **2015**, *6* (1), 7083.

(11) Kniepert, J.; Schubert, M.; Blakesley, J. C.; Neher, D. Photogeneration and Recombination in P3HT/PCBM Solar Cells Probed by Time-Delayed Collection Field Experiments. *J. Phys. Chem. Lett.* **2011**, *2* (7), 700−705.

(12) Maurano, A.; Shuttle, C. G.; Hamilton, R.; Ballantyne, A. M.; Nelson, J.; Zhang, W.; Heeney, M.; Durrant, J. R. Transient Optoelectronic Analysis of Charge Carrier Losses in a Selenophene/Fullerene Blend Solar Cell. *J. Phys. Chem. C* **2011**, *115* (13), 5947−5957.

(13) Clarke, T. M.; Lungenschmied, C.; Peet, J.; Drolet, N.; Mozer, A. J. A Comparison of Five Experimental Techniques to Measure Charge Carrier Lifetime in Polymer/Fullerene Solar Cells. *Adv. Energy Mater.* **2015**, *5* (4), No. 1401345.

(14) Albrecht, S.; Schindler, W.; Kurpiers, J.; Kniepert, J.; Blakesley, J. C.; Dumsch, I.; Allard, S.; Fostiropoulos, K.; Scherf, U.; Neher, D. On the Field Dependence of Free Charge Carrier Generation and Recombination in Blends of PCPDTBT/PC70BM: Influence of Solvent Additives. *J. Phys. Chem. Lett.* **2012**, *3* (5), 640−645.

(15) Hawks, S. A.; Finck, B. Y.; Schwartz, B. J. Theory of Current Transients in Planar Semiconductor Devices: Insights and Applications to Organic Solar Cells. *Physical Review Applied* **2015**, *3* (4), No. 044014.

(16) Kirchartz, T.; Nelson, J. Meaning of Reaction Orders in Polymer: Fullerene Solar Cells. *Phys. Rev. B* **2012**, *86* (16), No. 165201.

(17) Shuttle, C. G.; O'Regan, B.; Ballantyne, A. M.; Nelson, J.; Bradley, D. D.; Durrant, J. R. Bimolecular Recombination Losses in Polythiophene: Fullerene Solar Cells. *Phys. Rev. B* **2008**, *78* (11), No. 113201.

(18) Kirchartz, T.; Pieters, B. E.; Kirkpatrick, J.; Rau, U.; Nelson, J. Recombination via Tail States in Polythiophene: Fullerene Solar Cells. *Phys. Rev. B* **2011**, *83* (11), No. 115209.

(19) Blakesley, J. C.; Neher, D. Relationship Between Energetic Disorder and Open-Circuit Voltage in Bulk Heterojunction Organic Solar Cells. *Phys. Rev. B* **2011**, *84* (7), No. 075210.

(20) Rauh, D.; Deibel, C.; Dyakonov, V. Charge Density Dependent Nongeminate Recombination in Organic Bulk Heterojunction Solar Cells. *Adv. Funct. Mater.* **2012**, *22* (16), 3371−3377.

(21) Sandberg, O. J.; Tvingstedt, K.; Meredith, P.; Armin, A. Theoretical Perspective on Transient Photovoltage and Charge Extraction Techniques. *J. Phys. Chem. C* **2019**, *123* (23), 14261−14271.

(22) Deledalle, F.; Shakya Tuladhar, P.; Nelson, J.; Durrant, J. R.; Kirchartz, T. Understanding the Apparent Charge Density Dependence of Mobility and Lifetime in Organic Bulk Heterojunction Solar Cells. *J. Phys. Chem. C* **2014**, *118* (17), 8837−8842.

(23) Kiermasch, D.; Baumann, A.; Fischer, M.; Dyakonov, V.; Tvingstedt, K. Revisiting Lifetimes from Transient Electrical Characterization of Thin Film Solar Cells; A Capacitive Concern Evaluated for Silicon, Organic and Perovskite Devices. *Energy Environ. Sci.* **2018**, *11* (3), 629−640.

(24) Kay, A. M. Drift-Diffusion Simulator. *GitHub*, 2023. https://github.com/Austin-M-Kay/Drift_Diffusion_Simulator (accessed September 26th 2023).

(25) Sandberg, O. J.; Nyman, M.; Österbacka, R. Effect of Contacts in Organic Bulk Heterojunction Solar Cells. *Physical Review Applied* **2014**, *1* (2), No. 024003.

(26) Sandén, S.; Sandberg, O. J.; Xu, Q.; Smått, J. H.; Juška, G.; Lindén, M.; Österbacka, R. Influence of Equilibrium Charge Reservoir Formation on Photo-Generated Charge Transport in TiO2/Organic Devices. *Org. Electron.* **2014**, *15* (12), 3506−3513.

(27) Neukom, M. T.; Reinke, N. A.; Ruhstaller, B. Charge Extraction with Linearly Increasing Voltage: A Numerical Model for Parameter Extraction. *Sol. Energy* **2011**, *85* (6), 1250−1256.

(28) Hosseini, S. M.; Roland, S.; Kurpiers, J.; Chen, Z.; Zhang, K.; Huang, F.; Armin, A.; Neher, D.; Shoaee, S. Impact of Bimolecular Recombination on the Fill Factor of Fullerene and Nonfullerene-Based Solar Cells: A Comparative Study of Charge Generation and Extraction. *J. Phys. Chem. C* **2019**, *123* (11), 6823−6830.

(29) Sandberg, O. J.; Sundqvist, A.; Nyman, M.; Österbacka, R. Relating Charge Transport, Contact Properties, and Recombination to Open-Circuit Voltage in Sandwich-Type Thin-Film Solar Cells. *Physical Review Applied* **2016**, *5* (4), No. 044005.

(30) Armin, A.; Chen, Z.; Jin, Y.; Zhang, K.; Huang, F.; Shoaee, S. A Shockley-Type Polymer: Fullerene Solar Cell. *Adv. Energy Mater.* **2018**, *8* (7), No. 1701450.

(31) Kay, A. M. Recombination Rate Constant Corrector. *GitHub*, 2023. https://github.com/Austin-M-Kay/Recombination_Rate_Constant_Corrector (accessed September 26th 2023).

https://doi.org/10.1021/acs.jpclett.4c00218
J. Phys. Chem. Lett. 2024, 15, 4416−4421